IEEE Access
Multidisciplinary | Rapid Review | Open Access Journal

Received September 23, 2019, accepted October 16, 2019, date of publication October 21, 2019, date of current version November 1, 2019.

Digital Object Identifier 10.1109/ACCESS.2019.2948676

Phase Synchronization Information for Classifying Motor Imagery EEG From the Same Limb

BAOGUO XU[1], ZHIWEI WEI[1], AIGUO SONG[1], (Senior Member, IEEE), CHANGCHENG WU[2], DALIN ZHANG[1], WENLONG LI[1], GUOZHENG XU[3], HUIJUN LI[1], AND HONG ZENG[1]

[1]The State Key Laboratory of Bioelectronics, Jiangsu Key Lab of Remote Measurement and Control, School of Instrument Science and Engineering, Southeast University, Nanjing 210096, China
[2]College of Automation Engineering, Nanjing University of Aeronautics and Astronautics, Nanjing 211106, China
[3]College of Automation, Nanjing University of Posts and Telecommunications, Nanjing 210003, China

Corresponding author: Baoguo Xu (xubaoguo@seu.edu.cn)

This work was supported in part by the National Key Research and Development Program of China under Grant 2016YFB1001303, in part by the National Natural Science Foundation of China under Grant 61673114, Grant 91648206, Grant 61803201, and Grant 61673105, and in part by the Natural Science Foundation of Jiangsu Province under Grant BK20170803.

ABSTRACT The classification of motor imagery Electroencephalogram (EEG) of the same limb is important for natural control of neuroprosthesis. Due to the close spatial representations on the motor cortex area of the brain, the discrimination of the different motor imagery tasks is challenging. In this paper, phase synchronization information was proposed to classify motor imagery EEG within the same limb. In addition, non-portable was compared with portable EEG acquisition equipment for the purpose of making the brain computer interface (BCI) system more practical. In the non-portable case, the average accuracy of the binary classification and 3-class classification was 60.6% and 42.7%. In the portable case, the average EEG decoding accuracy of 58.5% and 39.9% was achieved for the two and three tasks. Furthermore, in both two cases, different sets of electrode pairs got the similar results. Moreover, we found that the proposed phase information based method was less sensitive to the number of EEG channels and had less performance degradation in portable EEG equipment. These results show it is possible to use phase synchronization information to discriminate different motor imagery tasks within the same limb. Eventually, this will potentially make the control of neuroprosthesis or other rehabilitation device more natural and intuitive.

INDEX TERMS Brain computer interface (BCI), motor imagery (MI), phase synchronization information.

I. INTRODUCTION

Since the 1970s, the brain-computer interface (BCI) system, especially the non-invasive BCI system, has made significant progress and has been widely used in medical rehabilitation and daily life [1]–[4]. It is well known that the key of the BCI system is classifying EEG signals to obtain corresponding commands to control external devices [5]. Obviously, the recognition accuracy of EEG signals directly affects the control performance of the BCI system. Therefore, feature extraction and classification of EEG signals play an important role in the development of the BCI system. So far, motor imagery EEG has been widely studied.

In [6], motor imagery EEG signals based on left hand, right hand, feet and tongue were applied to the BCI system. BCI-based neuroprosthesis control system was developed by using the imagination of repeated planar extension/flexion of both feet, or the imagination of repeated opening/closing left or right hand [7]. Mcfarland *et al.* controlled the movements of the cursor in three-dimensional space by imagining the movements of the left hand, right hand and feet [8]. The four-class BCI designed by Royer *et al.* allowed users to control the flight of a virtual helicopter in three-dimensional space. Users imagined their hands' movements and rest to control the forward and backward movements of the helicopter, and imagined their left and right hand's movements to control the helicopter to turn left and right [9].

However, traditional BCI system has the disadvantage of unnatural control and low control dimension. For example, a quadriplegic patient triggers a neuroprosthesis to complete the rehabilitation training by imagining the movements of the left hand, the right hand, the feet and the tongue.

The associate editor coordinating the review of this manuscript and approving it for publication was Nianqiang Li.

The movements in rehabilitation training are different from the imaginary movements, where patients use imaginary of foot's movements to control the hand's movements of neuroprosthesis [7]. From the patient's psychological point of view, this type of control is unnatural and will cause discomfort to the patient. In addition, the low control dimension of motor imagery BCI systems based on the left hand, right hand, feet, and tongue cannot satisfy the latest requirements for applications.

In order to solve these problems in the BCI system, it is of great importance to study EEG signals generated by imagining different movements from the same limb. In this way, users can use their own imaginary movements to control the corresponding movements of the neuroprosthesis and achieve natural control. Meanwhile, the classification of movement imagination EEG from the same limb can increase the control dimension of the BCI system.

In recent years, some studies had been carried out in this field. Yong and Menon used different algorithms to classify motor imagery EEG signals of the same upper limb, which included common spatial pattern (CSP), filter-bank CSP, logarithmic band power, linear discriminant analysis (LDA), logistic regression (LR) and support vector machine (SVM) [10]. Ofner *et al.* analyzed the encoding of the same upper limb movement in the time-domain from low-frequency EEG, and the average classification accuracy of imagined movement and movement was 27% [11]. Obviously, the classification of EEG signals from the same limb is very difficult, because these EEG signals contain very similar physiological changes in the brain and features [10]. As a result, more effective algorithms should be explored.

Most of the previous algorithms are based on the features derived from the power analysis on mu and beta rhythms [12]. However, phase information also plays an important role when different brain regions communicate with each other in cognitive tasks [13]. To the best of our knowledge, phase features have not been applied to the classification of motor imagery EEG of the same limb in the BCI literature.

In this research, phase synchronization information of the motor imagery EEG signals within the same limb was extracted as feature for the classification. At the same time, comparative study of non-portable and portable EEG acquisition equipment was carried out for the purpose of making the BCI system more practical. Furthermore, in both two cases, two sets of electrode pairs for achieving the phase synchronization information were studied. Discriminating different movement imagination EEG from the same limb will allow more natural and intuitive control of rehabilitation device (e.g. BCI-driven neuroprosthesis).

II. METHODS

A. EEG RECORDING

Eight healthy right-handed subjects volunteered to participate in our experiments (subject A to subject H), including four males and four females, aged between 24 and 26 years.

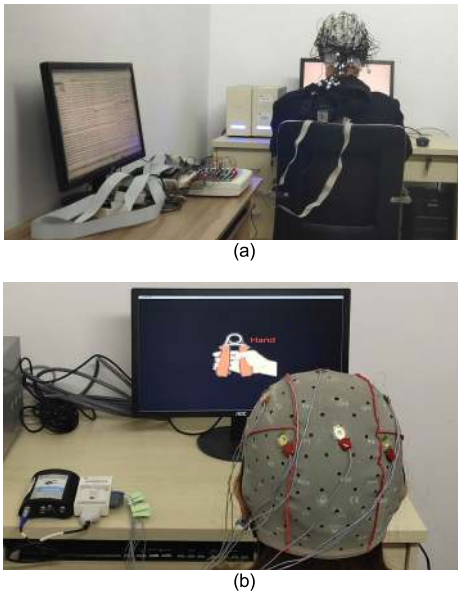

FIGURE 1. EEG acquisition equipment. (a) Non-portable EEG acquisition equipment. (b) Portable EEG acquisition equipment.

Three of them (subject C to subject E) used the non-portable equipment (Fig. 1(a)) for experiments, and all eight subjects conducted experiments with portable equipment (Fig. 1(b)). The same experiment paradigm was used for these two different EEG acquisition devices. Informed consent was obtained from all the participants. The experimental procedure was approved by the Ethics Committee of Medical College of Southeast University.

For non-portable equipment, we adopted SynAmps2 amplifier (Compumedics Neuroscan, USA) with a sampling frequency of 1000Hz. Twenty-seven electrodes were used: F1, Fz, F2, FC5, FC3, FC1, FCz, FC2, FC4, FC6, C5, C3, C1, Cz, C2, C4, C6, CP5, CP3, CP1, CPz, CP2, CP4, CP6, P1, Pz, and P2 (Fig. 2(a)). For portable equipment, g.MOBIlab+ amplifier (G.tec Medical Engineering GmbH, Austria) with a sampling frequency of 256Hz was utilized. Eight electrodes were chosen: FC3, FCz, FC4, C3, C4, P3, Pz, and P4 (Fig. 2(b)). For two kinds of equipment, left mastoid and Fpz were functioned as the reference electrode and the ground electrode, respectively. During the experiment, the amplifier automatically filtered out 50Hz power frequency interference in the signal, and the impedance of all electrodes was below 10kΩ.

B. EXPERIMENTAL PARADIGM

As illustrated in Fig. 3, four types of the motor imagery tasks were used in this study: (a) Rest (REST). (b) Movement imagination of grip with right hand (MI-HAND). (c) Movement imagination of Flexion/Extension with the right forearm (MI-FOREARM). (d) Movement imagination of reaching and grasping the target object with the right arm (MI-ARM).

The experimental paradigm is shown in Fig. 4. Each trial lasted 10 seconds. At t = 0s, a cross "+" was displayed for 1s to indicate the beginning of the trial. The next 1s was quiet.

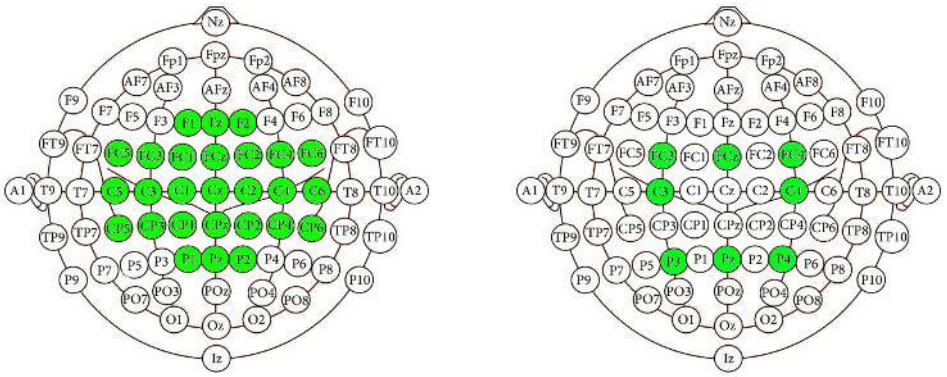

FIGURE 2. The EEG electrode positions in two acquisition devices. The electrodes shown in green were used in this study. (a) Electrodes used by non-portable acquisition devices. (b) Electrodes utilized by portable acquisition devices.

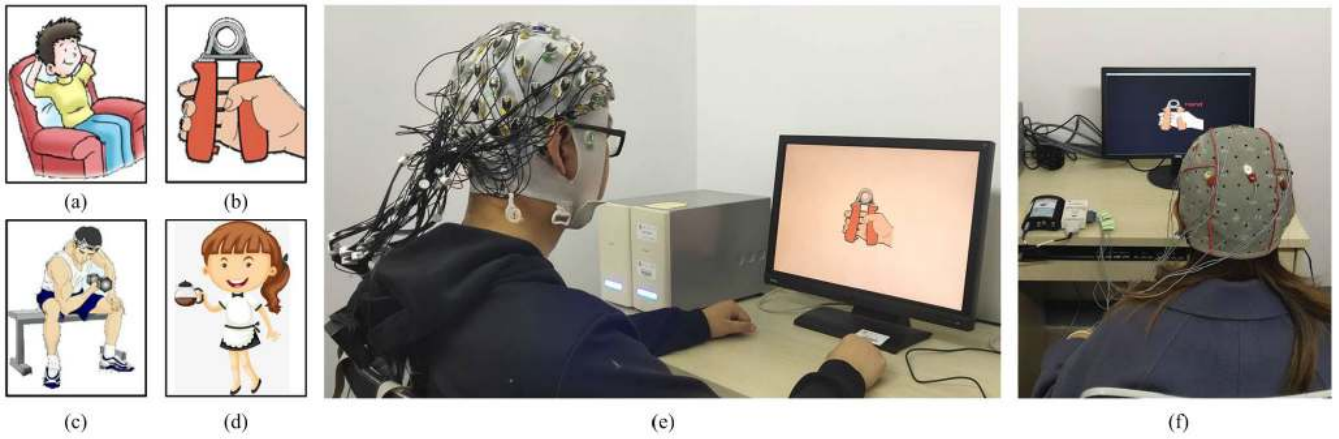

FIGURE 3. Different motor imagery tasks. (a) REST: The subjects were in a state of relaxation. (b) MI-HAND: Imagine using the grip with right hand. (c) MI-FOREARM: Imagine the right forearm flexion and extension. (d) MI-ARM: Imagine to reach-and-grasp the target object with the right arm. (e) An example of MI-HAND task with Non-portable equipment. (f) An example of MI-HAND task of with portable equipment.

At t = 2s, a motor imagery task cue was randomly presented, and the subjects performed corresponding movement imagination. From 6s to 10s, the subjects were in a relax state. The experiments consisted of 360 trials in which 90 trials for each type of motor imagery task.

C. PREPROCESSING

The EEG signal is a randomly non-stationary signal with low signal-to-noise ratio [14]. Through data preprocessing, background noise can be filtered to obtain EEG signals with high signal-to-noise ratio, which is very important for our subsequent data analysis.

In this study, time filtering and space filtering were used for data preprocessing. Firstly, linear phase FIR digital band-pass filter was chosen for time filtering in order to avoid phase distortion. The filtering frequency band of phase synchronization was 8-12Hz. Next, common average reference (CAR) method was used for space filtering. The CAR filter redefined the potential at each time t and at each electrode h by computing the mean value of the recorded signals of all H electrodes as the estimated reference point, as is shown in Eq.(1).

$$s'_h(t) = s_h(t) - \frac{1}{H}\sum_{i=1}^{H} s_i(t) \tag{1}$$

D. FEATURE EXTRACTION AND CLASSIFICATION

In neuroscience research, phase synchronization between signals is the key feature of information exchange between different cortex. Phase-locking value (PLV) is a measurement of phase synchronization in the time domain. In this study, PLV was used to extract phase information from EEG signals of different motor imagery from same limb. The calculation steps of PLV between two signals are generally as follows [12]-[14]:

Firstly, two signals are given, and their instantaneous phases are obtained by Hilbert transformation,

$$\mathrm{y}(t) = \frac{1}{\pi}\int_{-\infty}^{\infty}\frac{x(\tau)}{t-\tau}d\tau, \tag{2}$$

$$z(t) = x(t) + jy(t) = A(t)e^{j\theta(t)}, \tag{3}$$

FIGURE 4. Experimental paradigm.

where $y(t)$ is the Hilbert transform of $x(t)$, $z(t)$ is the analytic signal of $x(t)$, and $\theta(t)$ is the instantaneous phase of $x(t)$, j is the imaginary unit.

Secondly, the instantaneous phase difference between the two signals is achieved using the formula,

$$\theta(t) = \theta_1(t) - \theta_2(t). \tag{4}$$

Finally, PLV is calculated by instantaneous phase difference,

$$PLV = \frac{1}{N}\left|\sum_{t=1}^{N} \exp[j\theta(t)]\right|, \tag{5}$$

where N is the number of points used for calculation. The PLV ranges from 0 to 1, where 0 means no synchrony between two channels, and 1 means total synchrony between two channels [13].

According to [12], [14], there are two kinds of phase synchronization in the brain: large-scale and local-scale synchronization. Large-scale synchronization may exist between channels in different cerebral cortex, and local-scale synchronization may occur between adjacent channels in the same sensorimotor cortex. Recent study has demonstrated that using large-scale synchronization can achieve higher classification accuracy. Therefore, this study mainly focus on adopting large-scale phase synchronization to extract features from motor imagery EEG within the same limb.

In this research, large-scale synchronization was computed involving the following cerebral cortex: sensorimotor cortex (FC3, C3, CP3, P3, FC4, C4, CP4, and P4), and supplementary motor cortex (FCz, Cz, CPz, and Pz). In the non-portable case, two sets of electrode pairs were designed. As is shown in Fig. 5(a), the first set of electrode pairs are C3-FCz, FCz-C4, C4-CPz, CPz-C3, C3-C4 and FCz-CPz. The second set of electrode pairs are FC3-Cz, C3-Cz, CP3-Cz, FC4-Cz, C4-Cz and CP4-Cz, as illustrated in Fig. 5(b). Similarly, in the portable case, also two sets of electrode pairs were adopted. One set of electrode pairs are C3-FCz, FCz-C4, C4-Pz, Pz-C3, C3-C4 and FCz-Pz, as indicated in Fig. 5(c). Another set of electrode pairs are FC3-Pz, FC3-C4, FCz-P3, FCz-P4, FC4-C3 and FC4-Pz, as demonstrated in Fig. 5(d). The PLVs of six pairs of electrodes in each scheme were calculated and used as classification features.

Based on a lot of previous research, linear discriminant analysis (LDA) was chosen as classifier in this study. The core idea of the LDA algorithm is to project the sample into the optimal discriminant space to reduce the feature dimension and extract effective classification information.

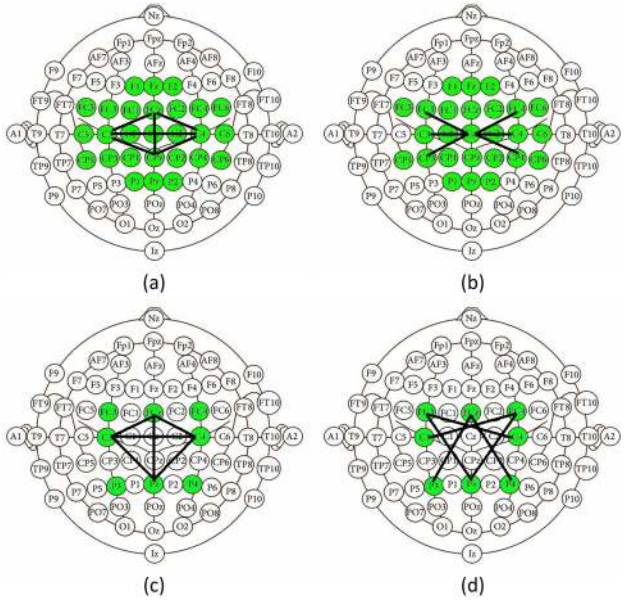

FIGURE 5. Large-scale synchronization electrode pairs. (a) and (b): Two sets of electrode pairs in non-portable case. (c) and (d): Two sets of electrode pairs in portable case.

The samples calculated by the LDA algorithm obtain the maximum inter-class distance and the minimum intra-class distance [15].

III. RESULTS

A. RESULTS BASED ON NON-PORTABLE EQUIPMENT

1) ERD/ERS ANALYSIS

Movement, preparation for movement and imagine movement are accompanied by changes in the energy of the relevant frequency bands in the brain. When people imagine movement, the energy of the mu rhythm (8-12Hz) and the beta (13-25Hz) rhythm on the contralateral sensorimotor cortex decrease, this phenomenon is called event-related desynchronizatio (ERD), which means the cortex is activated. By contrast, the energy of the mu rhythm and the beta rhythm on the ipsilateral sensorimotor cortex increase, which is called event-related synchronization (ERS), and the cortex is in an inert state at this time [16].

In this research, ERD analysis focused on energy changes of mu rhythm and beta rhythm in C3 channel. We used the EEG data between 1-8s from four types of motor imagery to calculate energy changes before and after motor imagery. The time = 0s in Fig. 6 was the starting point for movement imagination. It can be seen from Fig. 6 that when the brain was at rest, energy of mu rhythm and beta rhythm had not greatly changed. However, when the brain performed motor imagery, the contralateral energy of mu rhythm and beta rhythm decreased. Furthermore, the energy returned to its original level, when the motor imagery finished. In addition, the ERD phenomenon of subject C was more visible than subject E.

Additionally, EEGLAB toolbox was used to calculate the energy distribution of motor imagery EEG. Fig. 7(a) to

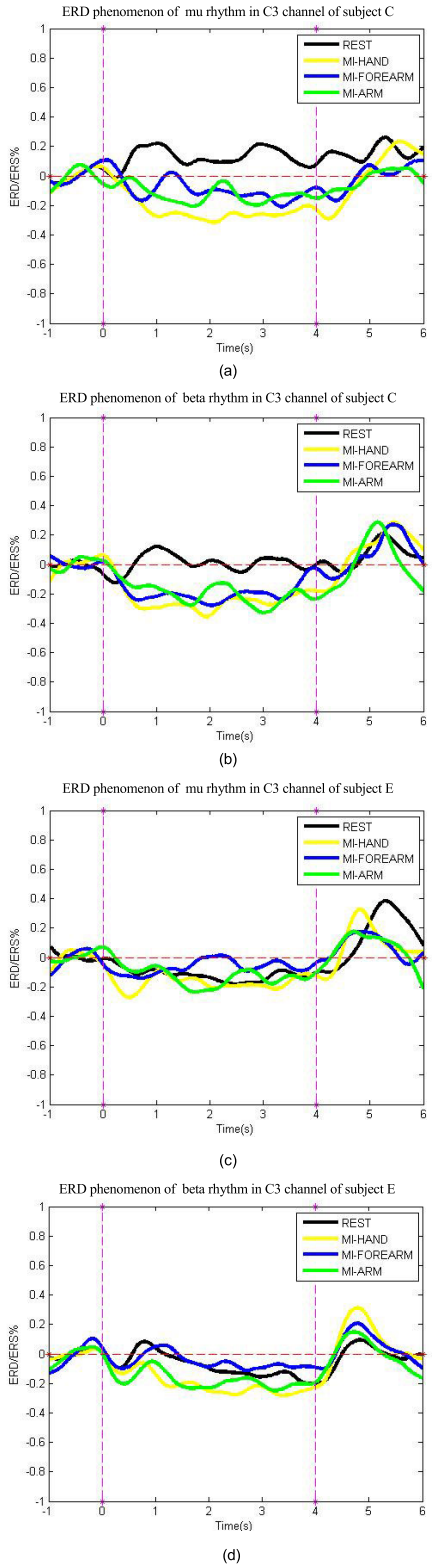

FIGURE 6. ERD phenomenon of C3 channel with mu rhythm (8-12Hz) and beta rhythm (13-25Hz). (a) and (b) are the results of subject C. (c) and (d) are the results of subject E.

Fig. 7(d) shows the brain topographic map of REST, MI-HAND, MI-FOREARM, and MI-ARM, respectively. It is obvious that the energy of mu rhythm on both sides of the

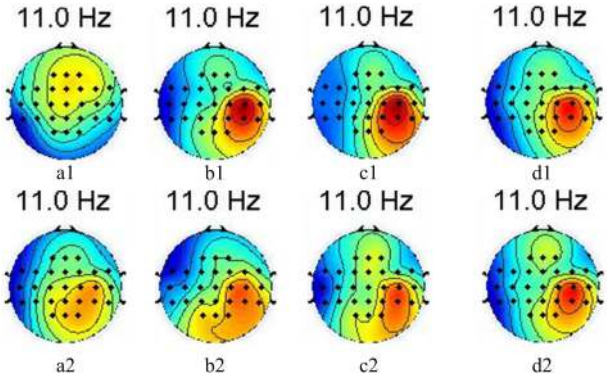

FIGURE 7. Brain topographic map. From a1 to d1 of subject C or a2 to d2 of subject E are the energy distribution of REST, MI-HAND, MI-FOREARM, and MI-ARM, respectively.

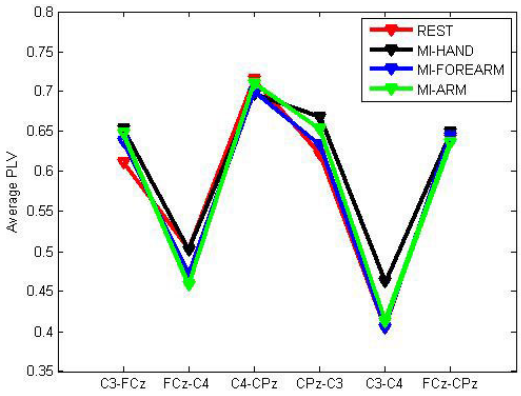

FIGURE 8. The average PLV of each of the four types of EEG on C3-FCz, FCz-C4, C4-CPz, CPz-C3, C3-C4, and FCz-CPz electrode pairs.

brain increases if the subjects are in a state of relaxation. By contrast, when subjects perform different motor imagery with the right limb, the energy of the left side of the brain decreases. Moreover, the energy changes are concentrated in the sensorimotor cortex.

2) RESULTS OF THE FIRST SET OF ELECTRODE PAIRS

Fig. 8 demonstrates the average PLV of each of the four types motor imagery EEG signals on C3-FCz, FCz-C4, C4-CPz, CPz-C3, C3-C4, and FCz-CPz electrode pairs, respectively. The average PLV was the average result of all the EEG data of the three subjects. The EEG signals between 2s and 6s were used for calculating the average PLV.

As illustrated in Fig. 8, three kinds of motor imagery EEG obtained higher average PLV on the C3-FCz and CPz-C3 electrode pairs, indicating that the phase synchronization of these electrode pairs increased when imagining right limb movement. Furthermore, the average PLV of the four types of EEG on the C3-FCz and CPz-C3 electrode pairs is easily distinguishable.

This study involved six kinds of binary classification combinations, i.e. REST vs MI-HAND, REST vs MI-FOREARM, REST vs MI-ARM, MI-HAND vs MI-FOREARM, MI-HAND vs MI-ARM, and MI-FOREARM vs MI-ARM, and four kinds of 3-class

TABLE 1. Classification accuracy of the first set of electrode pairs for non-portable equipment.

Subject	Classification Accuracy (%)									
	Binary Classification						3-class Classification			
	REST vs MI-HAND	REST vs MI-FOREARM	REST vs MI-ARM	MI-HAND vs MI-FOREARM	MI-HAND vs MI-ARM	MI-FOREARM vs MI-ARM	REST vs MI-HAND vs MI-FOREARM	REST vs MI-HAND vs MI-ARM	REST vs MI-FOREARM vs MI-ARM	MI-HAND vs MI-FOREARM vs MI-ARM
C	55.6	60.0	67.2	63.9	66.1	58.9	48.2	47.8	41.9	37.7
D	54.4	56.7	59.4	61.1	59.4	57.2	40.7	37.8	38.5	35.8
E	53.3	59.4	63.3	63.3	62.2	63.3	47.8	51.1	44.4	40.5
Mean	54.4	58.7	63.3	62.8	62.6	59.8	45.6	45.6	41.6	38.0

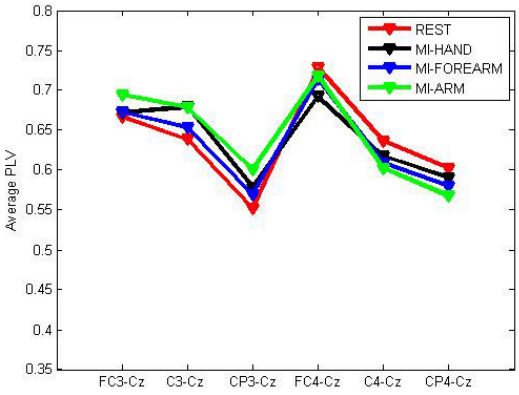

FIGURE 9. The average PLV of each of the four types of EEG on FC3-Cz, C3-Cz, CP3-Cz, FC4-Cz, C4-Cz, and CP4-Cz electrode pairs.

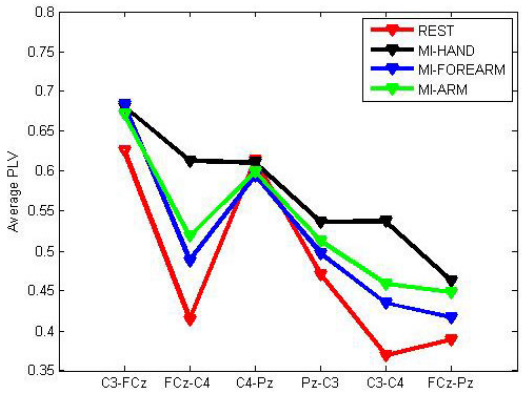

FIGURE 10. The average PLV of each of the four types of EEG on C3-FCz, FCz-C4, C4-Pz, Pz-C3, C3-C4, and FCz-Pz electrode pairs.

classification combinations, i.e. REST vs MI-HAND vs MI-FOREARM, REST vs MI-HAND vs MI-ARM, REST vs MI-FOREARM vs MI-ARM, and MI-HAND vs MI-FOREARM vs MI-ARM. The recognition accuracy was calculated using a window of 1s with step of 0.125s on 2-6s EEG signals.

As shown in Table 1, for the binary classification, the average accuracy is 60.3%. Furthermore, we obtained an average accuracy of 58.8% for classifying resting EEG against another type motor imagery EEG (REST vs MI-HAND, REST vs MI-FOREARM, and REST vs MI-ARM). Moreover, a mean classification accuracy between motor imagery tasks (MI-HAND vs MI-FOREARM, MI-HAND vs MI-ARM, and MI-FOREARM vs MI-ARM) was 61.7%. Moreover, for the 3-class classification, the average accuracy of 42.7% was achieved.

3) RESULTS OF THE SECOND SET OF ELECTRODE PAIRS

Fig. 9 illustrates the average PLV of each of the four types of motor imagery EEG on FC3-Cz, C3-Cz, CP3-Cz, FC4-Cz, C4-Cz, and CP4-Cz electrode pairs respectively. As demonstrated in Fig. 9, the resting EEG obtained the minimum PLV at FC3-Cz, C3-Cz, and CP3-Cz electrode pairs, and the maximum PLV achieved at FC4-Cz, C4-Cz, and CP4-Cz electrode pairs, indicating that the synchronization between the left hemisphere and the Cz electrode increased and the synchronization between the right hemisphere and the Cz electrode decreased, when imagining right limb movement. Also, the average PLV of the four types of EEG on the CP3-Cz and CP4-Cz electrode pairs can be easily distinguished.

According to the Table 2, the average accuracy for the binary classification is 60.6%. Moreover, the average accuracy between resting EEG and motor imagery EEG was 59.2%. Furthermore, we achieved an average accuracy of 61.9% for the motor imagery against another motor imagery. Thus, the classification algorithm based on phase synchronization information had better classification performance over the different motor imagery tasks without including REST task. This conclusion is consistent with the results of the first set of electrode pairs. For the 3-class classification, the mean classification accuracy was 42.1%.

B. RESULTS BASED ON PORTABLE EQUIPMENT

1) RESULTS OF THE FIRST SET OF ELECTRODE PAIRS

Average PLV of each of the four types of EEG on C3-FCz, FCz-C4, C4-Pz, Pz-C3, C3-C4, and FCz-Pz electrode pairs is shown in Fig. 10, respectively. The result was the average of all the EEG data from the eight subjects. As can be seen from the figure, three kinds of motor imagery EEG obtained higher average PLV on the C3-FCz and Pz-C3 electrode pairs, which was similar with those achieved in the first set of

TABLE 2. Classification accuracy of the second set of electrode pairs for non-portable equipment.

Subject	Classification Accuracy (%)									
	Binary Classification						3-class Classification			
	REST vs MI-HAND	REST vs MI-FOREARM	REST vs MI-ARM	MI-HAND vs MI-FOREARM	MI-HAND vs MI-ARM	MI-FOREARM vs MI-ARM	REST vs MI-HAND vs MI-FOREARM	REST vs MI-HAND vs MI-ARM	REST vs MI-FOREARM vs MI-ARM	MI-HAND vs MI-FOREARM vs MI-ARM
C	55.6	61.1	66.7	65.6	63.3	59.4	43.7	47.4	45.6	38.3
D	55.0	55.0	58.9	52.2	56.1	57.2	35.9	38.2	35.9	36.0
E	53.3	61.7	65.6	67.8	72.2	63.3	48.2	48.2	47.0	41.2
Mean	54.6	59.3	63.7	61.9	63.9	60.0	42.6	44.6	42.8	38.5

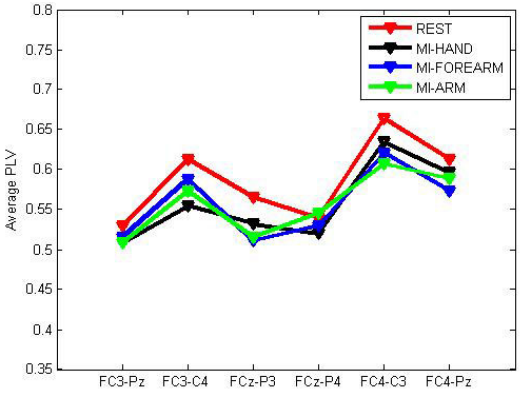

FIGURE 11. The average PLV of each of the four types of FC3-Pz, FC3-C4, FCz-P3, FCz-P4, FC4-C3, and FC4-Pz electrode pairs.

electrode pairs for non-portable case. Additionally, it is easy to differentiate the average PLV of the four types of EEG on the FCz-C4, Pz-C3, C3-C4, and FCz-Pz electrode pairs.

Table 3 shows the classification accuracy of eight subjects. For the binary classification, the average accuracy of 58.5% was got, and the average accuracy of the 3-class classification was 39.9%. By comparing the Table 3 to the Table 1, we can see that phase information based pattern recognition algorithm achieved similar classification accuracy in both the non-portable and portable scheme.

2) RESULTS OF THE SECOND SET OF ELECTRODE PAIRS

Fig.11 shows the average PLV of each of the four types of EEG on FC3-Pz, FC3-C4, FCz-P3, FCz-P4, FC4-C3, and FC4-Pz electrode pairs respectively. This set of electrodes connects different areas of cerebral cortex, which are far apart. As demonstrated in Fig. 11, the resting EEG obtained the maximum PLV at almost all of the electrode pairs. It can be seen that the average PLV of the four types of EEG on the FC3-C4 and FC4-C3 electrode pairs are easily distinguished. The mean accuracy of the binary classification and 3-class classification was 58.1% and 39.6%, as can be seen from the Table 4.

C. COMPARATIVE ANALYSIS OF CLASSIFICATION RESULTS

Fig. 12 and Fig. 13 show the phase information based classification results for the non-portable and portable respectively.

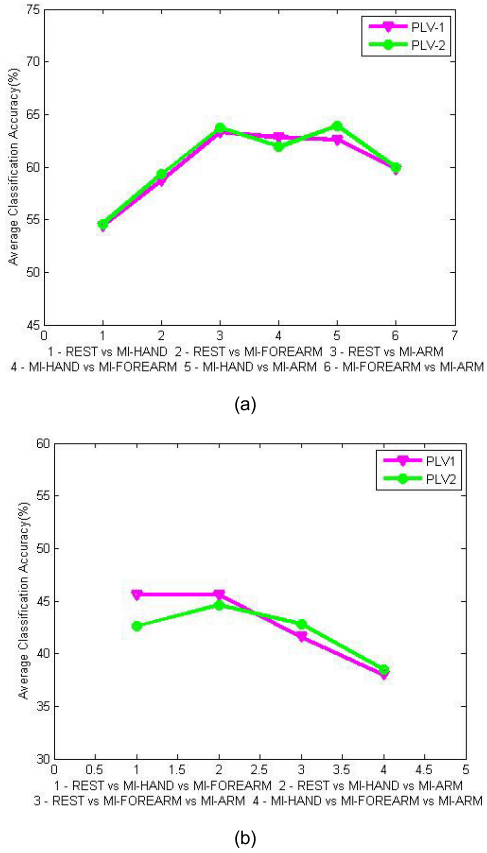

FIGURE 12. Non-portable classification results. (a) The result of binary classification. (b) The result of 3-class classification. PLV-1 and PLV-2 represent the result of the first set of electrode pairs and the second set of electrode pairs, respectively.

In the non-portable case, the first and second set of electrode pairs got the similar classification performance for both binary and 3-class classification except REST vs MI-HAND vs MI-FOREARM. In the portable case, we can achieve the similar conclusions.

Moreover, classic CSP method was used for comparison. Fig. 14 shows the average classification accuracy of the binary and 3-class classifications for different feature extraction methods under different EEG acquisition equipment.

In the case of non-portable, the algorithm based on spatial information was better than the algorithm based on phase syn-

TABLE 3. Classification accuracy of the first set of electrode pairs for portable equipment.

Subject	Classification Accuracy (%)									
	Binary Classification						3-class Classification			
	REST vs MI-HAND	REST vs MI-FOREARM	REST vs MI-ARM	MI-HAND vs MI-FOREARM	MI-HAND vs MI-ARM	MI-FOREARM vs MI-ARM	REST vs MI-HAND vs MI-FOREARM	REST vs MI-HAND vs MI-ARM	REST vs MI-FOREARM vs MI-ARM	MI-HAND vs MI-FOREARM vs MI-ARM
A	56.7	59.4	56.7	58.9	60.6	56.1	41.1	43.0	39.3	35.4
B	58.9	59.4	66.1	57.8	60.0	57.8	41.5	45.6	44.1	35.7
C	57.8	61.7	66.1	66.7	61.7	56.1	49.3	48.2	43.3	37.3
D	58.9	57.2	63.9	64.4	61.7	58.3	42.2	43.3	42.6	38.4
E	54.4	55.0	53.3	55.6	56.1	54.4	37.0	35.2	33.7	34.6
F	56.7	57.8	54.4	60.0	52.8	60.0	43.0	37.8	36.3	36.4
G	55.0	62.2	57.2	56.7	57.2	55.6	40.7	41.1	39.6	36.4
H	56.1	58.9	59.4	56.1	58.3	60.0	39.3	38.9	41.5	35.4
Mean	56.8	58.9	59.6	59.5	58.6	57.3	41.8	41.6	40.1	36.2

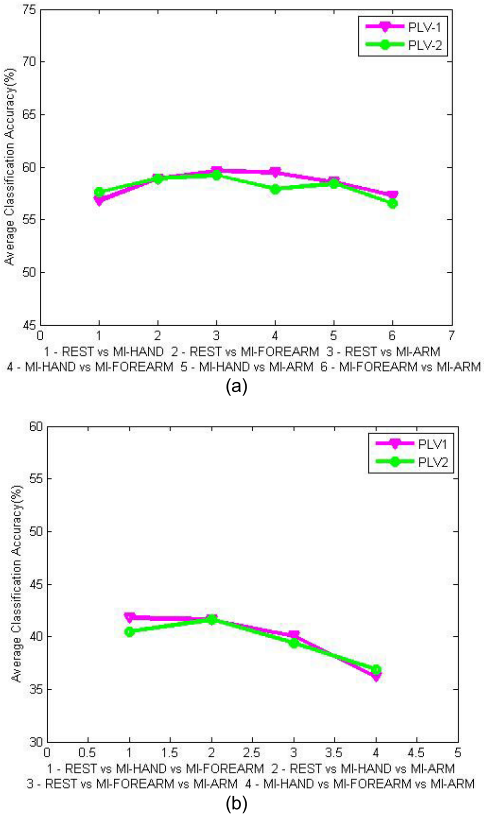

FIGURE 13. Portable classification result. (a) The result of binary classification; (b) The result of 3-class classification. PLV-1 and PLV-2 represent the result of the first set of electrode pairs and the second set of electrode pairs, respectively.

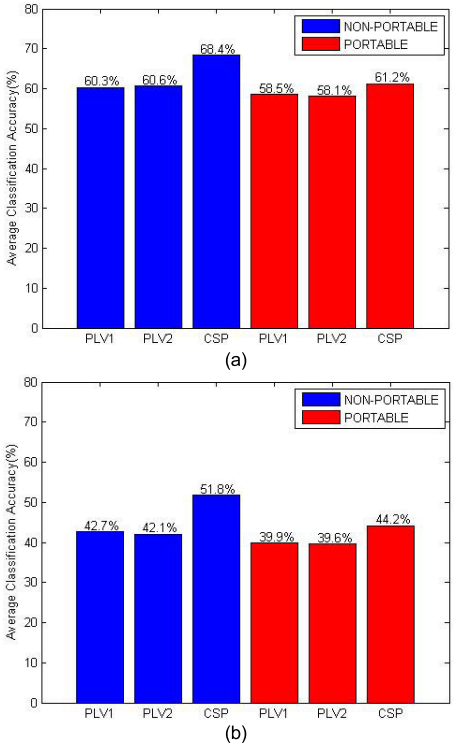

FIGURE 14. Binary and 3-class average classification accuracy of two sets of equipment under different algorithms. (a) The average accuracy of the binary classification. (b) The average accuracy of the 3-class classification. For both the non-portable and portable devices, the PLV1 and PLV2 represent the mean accuracy of the first set of electrode pairs and the second set of electrode pairs, respectively. CSP represents the average accuracy of classic CSP method.

chronization information, no matter it was binary or 3-class classification. The classification algorithm based on spatial information relied on multi-channel EEG data, and the number of data channels collected by non-portable equipment was larger and the spatial information was more obvious. Therefore, the non-portable algorithm based on spatial information achieved better classification results.

However, in the case of portable, the difference between spatial information based classification algorithm and phase information based algorithm become smaller. These results are consistent with those achieved in the literature [12].

In addition, from non-portable equipment to portable equipment, the spatial information based classification performance fell 7.2% and 7.6% for the binary and 3-class classifications, respectively. However, in the first set of electrode pairs, phase information based classification performance dropped only 1.8% and 2.8% for the binary and

TABLE 4. Classification accuracy of the second set of electrode pairs for portable equipment.

Subject	Classification Accuracy (%)									
	Binary Classification						3-class Classification			
	REST vs MI-HAND	REST vs MI-FOREARM	REST vs MI-ARM	MI-HAND vs MI-FOREARM	MI-HAND vs MI-ARM	MI-FOREARM vs MI-ARM	REST vs MI-HAND vs MI-FOREARM	REST vs MI-HAND vs MI-ARM	REST vs MI-FOREARM vs MI-ARM	MI-HAND vs MI-FOREARM vs MI-ARM
A	55.0	60.0	59.4	55.6	53.9	58.3	37.8	37.4	37.8	36.7
B	56.1	55.6	58.3	57.8	61.1	53.3	39.3	43.0	37.4	35.1
C	56.1	57.8	64.4	63.3	64.4	56.1	45.9	48.5	40.7	37.8
D	57.2	61.1	62.2	62.2	58.3	58.9	43.0	45.6	42.2	39.5
E	56.7	58.3	56.1	55.6	56.1	55.6	38.2	39.6	41.1	36.1
F	61.1	57.8	57.8	57.2	57.8	55.0	40.7	40.0	36.3	37.4
G	56.7	59.4	59.4	55.0	62.2	58.3	40.0	41.5	41.1	38.5
H	62.2	61.1	56.1	56.7	53.3	56.1	38.9	37.0	38.5	33.8
Mean	57.6	58.9	59.2	57.9	58.4	56.5	40.5	41.6	39.4	36.9

3-class classifications, respectively. In the second set of electrode pairs, phase information based classification performance decreased only 2.5% and 2.5% for the binary and 3-class classifications, respectively. In both sets of electrode pairs, phase information based method is less sensitive to the number of EEG channels and had obtained less performance degradation. This is of great importance in the BCI application, especially in BCI-driven neuroprosthesis.

Furthermore, based on our previous work [17], deep learning was also applied to extract and classify the features of the motor imagery EEG data. The average accuracy of the binary classification and 3-class classification in the non-portable and portable case was 62.6%, 44.3% and 61.4%, 42.4%. The deep learning algorithm also achieved less performance degradation from non-portable to portable. However, the deep learning algorithm takes a longer time to process the data, which is a disadvantage for online classification of motor imagery EEG signals. As a result, the phase synchronization information based classification algorithm is more suitable for the online application of BCI systems, such as EEG-based rehabilitation device and robot control system.

IV. DISCUSSION AND CONCLUSION

The motor imagery EEG signals of left hand, right hand, feet and tongue were used in traditional BCI system, which led to the problem of unnatural control and low control dimension, especially in prosthetic limb applications [7]–[9]. To some extent, these problems can be solved by adopting motor imagery EEG with the same limb. However, the physiological features of these EEG signals are very similar, which brings a great challenge to feature extraction and classification.

In most studies on the classification of motor imagery EEG from the same limb, researchers mainly adopted the algorithm based on the energy change of mu rhythm and beta rhythm, and seldom considered the phase information of the EEG signals [10], [11]. However, phase has been also an important feature to distinguish motor imagery EEG.

In this study, synchronization phase information was proposed to extract the features from the motor imagery EEG of the same limb. Different sets of electrode pairs were used to calculate the PLV. In addition, non-portable equipment can collect more channels of EEG data with high sampling frequency. However, its experimental procedure is cumbersome and the equipment is large, which is not suitable for the BCI application in daily life. By contrast, portable equipment is small in size and easy to carry. Furthermore there are fewer channels to collect EEG, and the sampling frequency is relatively low. However, it is convenient to use portable equipment for the application of BCI driven system.

For this reason, comparative study on both on-portable and portable equipment were conducted. The proposed phase synchronization information based method, the classic CSP method, and the wavelet transform time-frequency image and convolutional network based method was used to classify the movement imagination EEG with the same limb. However, phase information based method was less sensitive to the number of EEG channels and had obtained less performance degradation. Moreover, the proposed phase information based method satisfies online BCI application, due to its low complexity.

These findings are very significative for the BCI application, particularly in the natural and intuitive control of upper limb neuroprostheisis or other multi-degree-of-freedom robot.

REFERENCES

[1] S. Kalagi, J. Machado, V. Carvalho, F. Soares, and D. Matos, "Brain computer interface systems using non-invasive electroencephalogram signal: A literature review," in *Proc. Int. Conf. Eng., Technol. Innov. (ICE/ITMC)*, Jun. 2017, pp. 1578–1583.

[2] A. A. Frolov, O. Mokienko, R. Lyukmanov, E. Biryukova, S. Kotov, L. Turbina, G. Nadareyshvily, and Y. Bushkova, "Post-stroke rehabilitation training with a motor-imagery-based brain-computer interface (BCI)-controlled hand exoskeleton: A randomized controlled multicenter trial," *Frontiers Neurosci.*, vol. 11, Jul. 2017.

[3] R. Mohanty, A. M. Sinha, A. B. Remsik, K. C. Dodd, and B. M. Young, "Machine learning classification to identify the stage of brain-computer interface therapy for stroke rehabilitation using functional connectivity," *Frontiers Neurosci.*, vol. 11, p. 400, May 2018.

[4] R. Zhang, Y. Li, Y. Yan, H. Zhang, S. Wu, T. Yu, and Z. Gu, "Control of a wheelchair in an indoor environment based on a brain–computer interface and automated navigation," *IEEE Trans. Neural Syst. Rehabil. Eng.*, vol. 24, no. 1, pp. 128–139, Jan. 2015.
[5] D. J. McFarland and J. R. Wolpaw, "Brain–computer interface use is a skill that user and system acquire together," *PLoS Biol.*, vol. 16, no. 7, Jul. 2018, Art. no. e2006719.
[6] W.-Y. Hsu, "Fuzzy Hopfield neural network clustering for single-trial motor imagery EEG classification," *Expert Syst. Appl.*, vol. 39, no. 1, pp. 1055–1061, Jan. 2012.
[7] A. Schwarz, P. Ofner, J. Pereira, A. I. Subrlea, and G. R. Müller-Putz, "Decoding natural reach-and-grasp actions from human EEG," *J. Neural Eng.*, vol. 15, no. 1, Dec. 2017, Art. no. 016005.
[8] D. J. McFarland, W. A. Sarnacki, and J. R. Wolpaw, "Electroencephalographic (EEG) control of three-dimensional movement," *J. Neural Eng.*, vol. 7, no. 3, May 2010, Art. no. 036007.
[9] A. S. Royer, A. J. Doud, M. L. Rose, and B. He, "EEG control of a virtual helicopter in 3-dimensional space using intelligent control strategies," *IEEE Trans. Neural Syst. Rehabil. Eng.*, vol. 18, no. 6, pp. 581–589, Dec. 2010.
[10] X. Yong and C. Menon, "EEG classification of different imaginary movements within the same limb," *PLoS ONE*, vol. 10, no. 4, Apr. 2015, Art. no. e0121896.
[11] P. Ofner, A. Schwarz, J. Pereira, and G. R. Müller-Putz, "Upper limb movements can be decoded from the time-domain of low-frequency EEG," *PLoS ONE*, vol. 12, no. 8, Aug. 2017, Art. no. e0182578.
[12] Y. Wang, B. Hong, X. Gao, and S. Gao, "Phase synchrony measurement in motor cortex for classifying single-trial EEG during motor imagery," in *Proc. Int. Conf. IEEE Eng. Med. Biol. Soc.*, Aug. 2006, pp. 75–78.
[13] B. Xu, Y. Fu, G. Shi, X. Yin, Z. Wang, and H. Li, "Phase information for classification between clench speed and clench force motor imagery," *Sensors Transducers*, vol. 170, no. 5, pp. 234–240, May 2014.
[14] A. Loboda, A. Margineanu, G. Rotariu, and A. M. Lazar, "Discrimination of EEG-based motor imagery tasks by means of a simple phase information method," *Int. J. Adv. Res. Artif. Intell.*, vol. 3, no. 10, pp. 11–15, Oct. 2014.
[15] R. Varatharajan, G. Manogaran, and M. K. Priyan, "A big data classification approach using LDA with an enhanced SVM method for ECG signals in cloud computing," *Multimedia Tools Appl.*, vol. 77, no. 8, pp. 10195–10215, Apr. 2018.
[16] G. Pfurtscheller and F. H. L. da Silva, "Event-related EEG/MEG synchronization and desynchronization: Basic principles," *Clin. Neurophysiol.*, vol. 110, no. 11, pp. 1842–1857, Nov. 1999.
[17] B. Xu, L. Zhang, A. Song, C. Wu, W. Li, D. Zhang, G. Xu, H. Li, and H. Zeng, "Wavelet transform time-frequency image and convolutional network-based motor imagery EEG classification," *IEEE Access*, vol. 7, pp. 6084–6093, 2018.

BAOGUO XU was born in Nantong, China, in 1981. He received the B.S. degree in measurement and control from the China University of Mine and Technology, Xuzhou, China, in 2004, and the Ph.D. degree in measurement and control from Southeast University, Nanjing, China, in 2009. He is currently an Associate Professor with the School of Instrument Science and Engineering, Southeast University. His current research interests include brain–computer interface, natural human–robot interaction, and rehabilitation robot.

ZHIWEI WEI was born in Shanxi, China, in 1993. He received the B.S. degree in measurement and control technology and instrument from Yanshan University, Qinhuangdao, China, in 2017. He is currently pursuing the M.S. degree in instrument and meter engineering with Southeast University, Nanjing, China. His current research interests include motor imagery EEG analysis and machine learning.

AIGUO SONG was born in Huangshan, China, in 1968. He received the B.S. degree in automatic control and the M.S. degree in measurement and control from the Nanjing University of Aeronautics and Astronautics, Nanjing, China, in 1990 and 1993, respectively, and the Ph.D. degree in measurement and control from Southeast University, Nanjing, China, in 1996. From 1996 to 1998, he was an Associate Researcher with the Intelligent Information Processing Laboratory, Southeast University. From 1998 to 2000, he was an Associate Professor with the Department of Instrument Science and Engineering, Southeast University. From 2000 to 2003, he was the Director of the Robot Sensor and Control Laboratory, Southeast University. From 2003 to 2004, he was a Visiting Scientist with the Laboratory for Intelligent Mechanical Systems, Northwestern University, Evanston, IL, USA. He is currently a Professor with the School of Instrument Science and Engineering, Southeast University. His current research interests include teleoperation, haptic display, Internet telerobotics, and distributed measurement systems.

CHANGCHENG WU was born in Liancheng, China, in 1987. He received the B.S. degree in measurement and control from Jilin University, Changchun, China, in 2010, and the Ph.D. degree in instrument science and technology from Southeast University, Nanjing, China, in 2016. He is currently a Lecturer with the College of Automation Engineering, Nanjing University of Aeronautics and Astronautics. His current research interests include human–robot interaction and robotic control.

DALIN ZHANG was born in Henan, China, in 1995. He received the B.S. degree in measurement and control technology from Henan University, Kaifeng, China, in 2018. He is currently pursuing the M.S. degree in instrument science and technology with the Southeast University, Nanjing, China. His current research interests include brain–computer interface and machine learning.

WENLONG LI was born in Henan, China, in 1995. He received the B.S. degree in measurement and control technology from Zhengzhou University, Zhengzhou, China, in 2018. He is currently pursuing the M.S. degree in instrument science and technology with the Southeast University, Nanjing, China.

His current research interests include brain–computer interface and human–robot interaction.

GUOZHENG XU received the B.S. degree in mechatronics from Anhui Polytechnic University, Wuhu, China, in 2002, the M.S. degree in mechatronics from the Nanjing University of Aeronautics and Astronautics, Nanjing, China, in 2005, and the Ph.D. degree in instrumental science and technology from Southeast University, Nanjing, China, in 2010. He is currently an Associate Professor with the College of Automation and Artificial Intelligence, Nanjing University of Posts and Telecommunications, Nanjing. His current research interests include rehabilitation robot and human–robot interaction.

HUIJUN LI was born in Pingdingshan, China, in 1976. She received the B.S. degree in instrument science and the M.S. degree in condensed matter physics from Zhengzhou University, Zhengzhou, China, in 1999 and 2002, respectively, and the Ph.D. degree in measurement and control from Southeast University, Nanjing, China, in 2005. She is currently an Associate Professor with the School of Instrument Science and Engineering, Southeast University. Her current research interests include teleoperation and rehabilitation robotics.

HONG ZENG was born in Langzhong, China, in 1981. He received the M.E. degree in signal and information processing from the Radio Department, Southeast University, in 2006, and the Ph.D. degree from the Department of Computer Science, Hong Kong Baptist University, in 2010. He is currently an Associate Professor with the School of Instrument Science and Engineering, Southeast University. His current research interests include machine learning, pattern recognition, and bio-signal processing.